

Fringe-Field Driven Single-Gap and Single-Gamma Transflective Liquid Crystal Display with Dual Orientation of Liquid Crystal

Min Oh CHOI, Eun JEONG, Mi Hyung CHIN, Young Jin LIM, Kyoung-Mi KIM¹, Gi-Dong LEE^{1*}, and Seung Hee LEE[†]

Polymer BIN Fusion Research Center, School of Advanced Materials Engineering, Chonbuk National University, Chonju, Chonbuk 561-756, Korea

¹*Department of Electronics Engineering, Dong-A University, Pusan 607-735, Korea*

(Received September 11, 2007; revised October 12, 2007; accepted November 1, 2007; published online November 30, 2007)

The fringe electric field-driven transflective nematic liquid crystal display with dual orientation has a problem that the voltage-dependent transmittance and reflectance curves do not match each other, requiring a dual driving circuit to achieve a high electro-optic performance. Optimizations of the electrode structure in the array substrate and configuration of each optical layer solve this problem so that the transflective display with a single-gap and a single-gamma curve is possible.

[DOI: [10.1143/JJAP.46.L1164](https://doi.org/10.1143/JJAP.46.L1164)]

KEYWORDS: transflective liquid crystal display, fringe-field, electrode structure

Recently, transflective liquid crystal displays (LCDs) are becoming more and more important due to its increasing use in portable displays which requires a good visibility under any lighting conditions.¹⁾ So far various types of transflective LCDs have been developed^{2–4)} satisfying the conditions for good visibility. One of drawbacks of conventional transflective displays was narrow viewing angle because the liquid crystal (LC) director tilts up in one direction in the transmissive mode. In order to solve such a low image quality problem, homogeneously aligned LC transflective cells driven by fringe electric field [named fringe-field switching (FFS)]^{5,6)} with a dual cell gap in which the LC director rotates almost in plane was proposed. However, this device is difficult to manufacture due to the different cell gaps in the transmissive (T) and reflective (R) regions. In addition, the voltage-dependent reflectance and transmittance curves do not match each other. Consequently, two driving circuits for the R- and T-regions are required to realize a high image quality.

To overcome the dual cell gap problem, a single-cell gap cell structure was reported, in which the LC has a hybrid alignment in the R-region and a homogeneous alignment in the T-region.⁷⁾ However, there is still a significant difference in the electrooptic curves such as voltage-dependent luminance between the R- and T-regions. In the device, the operation voltage (V_{op}) defined as a voltage that generates 98% of maximal transmittance for T-region does not coincide with operation voltage for R-region and is much higher than in the R-region. This is due to the fact that the LC in top substrate of the R-region is anchored vertically without bias in azimuthal anchoring. In order to solve this problem, we investigate the cell configuration including optical and electrode structures in which the voltage dependent reflectance and transmittance matches.

Figure 1 shows a schematic cell structure of the dual orientation transflective display driven by fringe-electric field. In the R-region, the LC has a hybrid alignment compared to T-region which has a homogeneous alignment. Owing to hybrid alignment in the R-region, the effective cell retardation value becomes half of real cell retardation value. The R-region consists of one polarizer, $\lambda/2$ film, hybrid

aligned LC with an effective retardation value of $\lambda/4$ and a reflector. In the T-region, a mirror image method is applied against R-region configuration such that it consists of two parallel polarizers, two $\lambda/2$ films and a homogeneous aligned LC layer with $\lambda/2$. And the direction of the slit electrode with electrode width (w) and distance (l) between them is 70° with respect to the LC layer in both R- and T-regions.

With this structure, normally black mode is realized for both regions. More specifically, we used Poincare sphere representation to understand a polarization path change of this single cell-gap transflective LCDs, as shown in Fig. 2. For the R-region, in the absence of voltage, the linearly polarized light (P1) moves to another linearly polarized light state (P3) through $\lambda/2$ film (P2) and transformed to a circularly polarized light state (P4) through the LC director (P5) with an effective cell retardation value of $\lambda/4$. The light reflecting from the reflector passes through $\lambda/4$ LC layer and then becomes linearly polarized light (P6). The linearly polarized light again passes through $\lambda/2$ film (P2), resulting in linearly polarized state (P7) opposite to the original input beam giving rise to a dark state, as shown in the Poincare sphere of Fig. 2(a). With the bias voltage, the LC director is assumed to rotate by 45° . Here, the linearly polarized light (P1) becomes to another linearly polarized light state (P3) through $\lambda/2$ film (P2) and then propagates along the fast axis of the LC director (P4) without changing polarization state. The light reflected from the reflector propagates through LC director again, without changing polarization state. This light (P3) moves to original input linearly polarized light state (P1) through $\lambda/2$ film (P2), resulting in a bright state, as described in Fig. 2(b). Considering T-region, in the absence of voltage, the linearly polarized light (P1) moves to another linearly polarized light state (P3) through $\lambda/2$ film (P2) and then encounter LC director (P4) with an effective cell retardation value of $\lambda/2$ making an angle of 45° between the LC director and the polarized light. Then, the optic axis of input light rotates to linearly polarized light state (P5) facing $\lambda/2$ film (P2) again, and thus it becomes another linearly polarized light state (P6) which is in opposite to original polarized state, resulting in dark state, as shown in Fig. 2(c). With the bias voltage, the LC director rotates by 45° so the linearly polarized light (P1) becomes another linearly polarized light state (P3) through $\lambda/2$ film (P2) and then passes the LC director (P4) along a fast axis of

*E-mail address: gdllee@dau.ac.kr

†E-mail address: Ish1@chonbuk.ac.kr

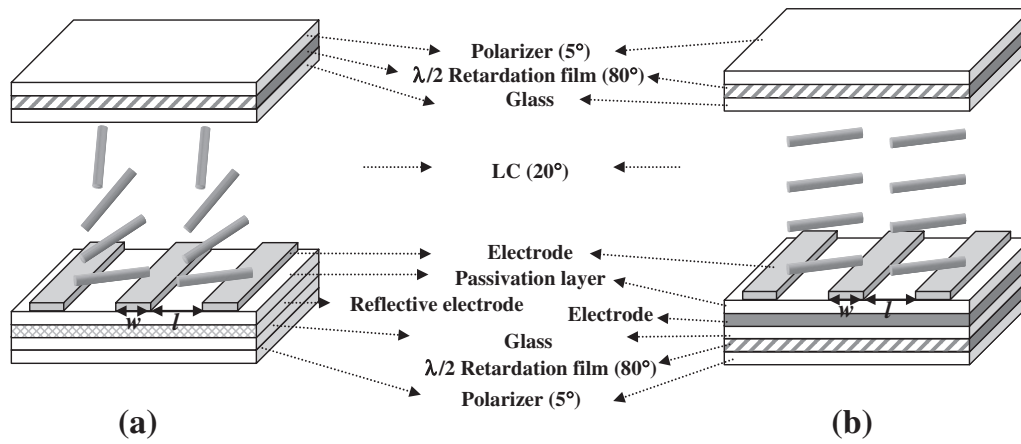


Fig. 1. Optical configuration of the single gap transfective LCDs used for simulation in the proposed device: (a) R- and (b) T-regions. The values in parentheses indicate optic axes of each optic layer with respect to horizontal direction.

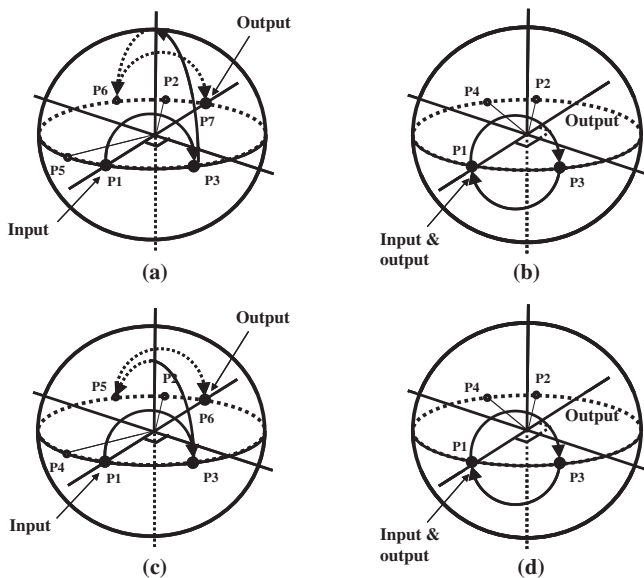


Fig. 2. Poincare sphere representation of the polarization path: (a) dark and (b) white states in the R-region, and (c) dark and (d) white states in the T-region.

LC director, without changing polarization state. Finally, it faces $\lambda/2$ film (P2) and then it returns to original polarized state (P1), resulting in white state, as shown in Fig. 2(d).

To investigate the device's electro-optic characteristics for above mentioned conditions, we performed a computer simulation using the commercially available software, "LCD Master" (Shintech, Japan). The motion of the LC director is calculated based on the Eriksen-Leslie theory⁸⁾ and 2×2 extended Jones matrix is applied for the optical transmittance calculation. The transmittance for the single and parallel polarizers was assumed to be 41 and 35%, respectively. For the calculation, an LC with a birefringence of 0.070 at 550 nm and a dielectric anisotropy of -4.0 was used. The cell gap (d) was $4.0 \mu\text{m}$.

Previously, optimization of cell parameters such as w , l and rubbing angle was performed in a fringe-field driven homogeneously aligned transfective liquid crystal cell to achieve a single gamma curve.⁹⁾ Similar approach was performed in this device. Figure 3 shows how the electrode structure affects the V_{op} , transmittance and reflectance. To

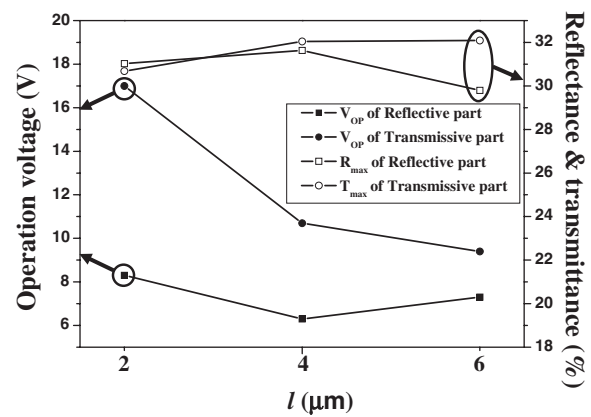


Fig. 3. Maximum reflectance, transmittance, and operation voltages of each region as a function of electrode width and distance.

determine a condition for the matched electro-optic characteristics of R- and T-regions, w is fixed as $4.0 \mu\text{m}$ and l was varied from 2.0 to $6.0 \mu\text{m}$. As indicated, the V_{op} for T-region decreases. This is due to the fact that with increasing l the intensity of horizontal field component increases, which rotates the LC more effectively. On the other hand, the electrode condition to match the V_{op} of T-region in the R-region was $w = 4 \mu\text{m}$ and $l = 2 \mu\text{m}$. With these conditions, the difference in the V_{op} between two regions is small and transmittance and reflectance are quite good. However, we found that in the electrode condition with $w = 4.0 \mu\text{m}$ and $l = 4.0 \mu\text{m}$ for T-region, the reflectance and transmittance difference in mid-grey level is smaller than that of the cell with the condition of $w = 4.0 \mu\text{m}$ and $l = 6.0 \mu\text{m}$. Therefore, the electrode condition with $w = 4.0 \mu\text{m}$ and $l = 4.0 \mu\text{m}$ for T-region and $w = 4.0 \mu\text{m}$ and $l = 2.0 \mu\text{m}$ for R-region was chosen. Figure 4 shows normalized voltage-dependent transmittance and reflectance with the optimized electrode condition. As indicated, both curves match perfectly so that a single driving circuit can control displayed images in both the R- and T-regions, realizing the transfective display with single-gap and single-gamma driving.

Finally, viewing angle characteristics of the device is analyzed. In the R- and T-regions, the region in which the contrast ratio is greater than 5 exists at a polar angle of more than almost 50° in all direction as shown in Fig. 5.

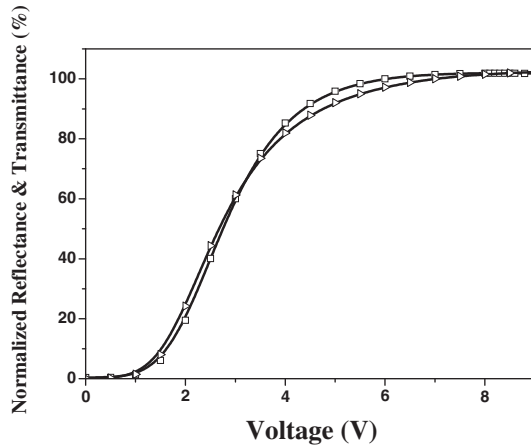


Fig. 4. Normalized voltage-dependent reflectance and transmittance curves in the proposed cell when the incident light is 550 nm (square: R-region, triangle: T-region).

In summary, we have studied optimal optical cell configuration and electrode condition for the fringe-field driven transfective display with dual orientation to achieve single-gap and single-gamma driving circuit. The optimized results show a perfectly matching voltage-dependent transmittance and reflectance curves with wide viewing angle.

This research was supported by the Ministry of Education and Human Resources Development (MOE), the Ministry of Commerce, Industry and Energy (MOCIE), and the Ministry of Labor (MOLAB) through the fostering project of the Lab of Excellency.

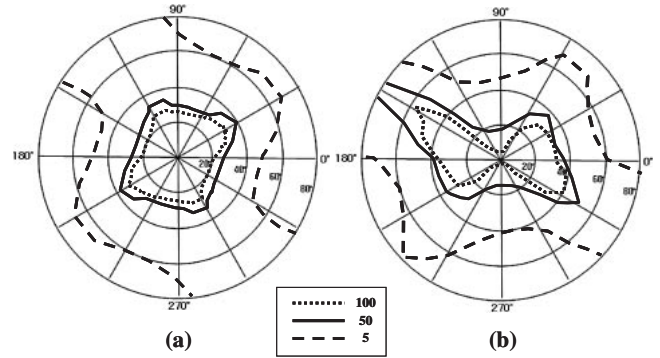


Fig. 5. Iso-contrast contour at an incident wavelength of 550 nm for the (a) R- and (b) T-regions in the proposed cell.

- 1) H.-I. Baek, Y.-B. Kim, K.-S. Ha, D.-G. Kim, and S.-B. Kwon: Proc. Int. Display Workshops'00, 2000, p. 41.
- 2) M. Jisaki and H. Yamaguchi: Proc. Int. Display Workshops'01, 2001, p. 133.
- 3) E. Yoda, T. Uesaka, T. Ogasawara, and T. Toyooka: SID Int. Symp. Dig. Tech. Pap. **33** (2002) 762.
- 4) S. H. Lee, H. W. Do, G.-D. Lee, T.-H. Yoon, and J. C. Kim: *Jpn. J. Appl. Phys.* **42** (2003) L1455.
- 5) T. B. Jung, J. H. Song, D.-S. Seo, and S. H. Lee: *Jpn. J. Appl. Phys.* **43** (2004) L1211.
- 6) J. B. Park, H. Y. Kim, Y. H. Jeong, D. H. Lim, S. Y. Kim, Y. J. Lim, and S. H. Lee: *Jpn. J. Appl. Phys.* **44** (2005) 6695.
- 7) Y. J. Lim, J. H. Song, and S. H. Lee: *Jpn. J. Appl. Phys.* **44** (2005) 3080.
- 8) E. B. Priestley, P. J. Wojtowicz, and P. Sheng: *Introduction to Liquid Crystals* (Plenum, New York, 1979).
- 9) Y. J. Lim, M.-H. Lee, G. D. Lee, W.-G. Jang, and S. H. Lee: *J. Phys. D* **40** (2007) 2759.